Data-Driven Evaluation of Endo-Clutter Detectors for Cognitive Radars

Pierre Bruneel, Milan Rozel

Data-Driven Evaluation of Endo-Clutter Detectors for Cognitive Radars

Pierre BRUNEEL
DEMR, ONERA, Université de Paris-Saclay, Palaiseau
FRANCE
pierre.bruneel@onera.fr

Milan ROZEL
DEMR, ONERA, Université de Paris-Saclay, Palaiseau
FRANCE
milan.rozel@onera.fr

ABSTRACT

In this paper, we use several degrees of freedom (central frequency and polarization of the radar waveform) in order to characterize the clutter signature. We study the properties of the covariance matrix of the clutter returns using a multi-dimensional representation of the signal inside a specific clutter cell. We measure clutter returns with an S-band ground radar using multiple waveforms in order to obtain this multi-dimensional representation. We study how the nature of the degrees of freedom included in the signature affects the properties of the covariance matrix of the clutter cell using an effective rank analysis. Eventually, we address the false alarm problem with the following question: how long is the estimation of the clutter covariance matrix valid. To do so, we empirically estimate the covariance matrices of the clutter at different instants, and generate synthetic clutter returns following these distributions. A detector based on a previous covariance matrix evaluates the impact on the false alarm rate of this mismatch.

1.0 INTRODUCTION

Unmanned Aerial Vehicles (UAV) are a rapidly growing threat in modern warfare. Due to their low cost and small size, they can play very different roles in the battlefield, be it surveillance, logistics or weapon-like usage. The detection and interception of these UAVs is very challenging even for modern equipment. Radars are commonly used to detect fighters or missiles and thus have trouble in the detection of UAV due to their small size, their low speed and their ability to fly close to the ground [1]. The strong returns of the ground clutter are a known problem for ground radars, and are often tackled by discarding a vast part of the Doppler-range data, a data that may include low-speed UAV signal. The usage of the micro-Doppler signature of the UAV presenting rotating blades is a proposition to discriminate the signature of the UAV against clutter or birds [2], [3]. However, it necessitates heavy computation and training as well as a strong signal to noise ratio (SNR) in order to be able to operate, and the blades can be made in low-reflecting materials or concealed. The complete analysis of a scene requires following the UAVs even at low speed, where they can hide in the clutter, hence the discrimination between the target and clutter signature is essential for detection. One the one hand, this involves the characterization of the signature of the ground clutter [4], [5], [6], which is a challenging task since ground clutter is a complex domain hat regroups scatterers with various timescales of fluctuations. On the other hand, several experiments report measurements of the signature of UAVs' radar signature as a function of frequency or polarization of the electromagnetic wave in anechoic chambers [7]. The new capabilities of computers and software-defined radio allow the advent of concepts such as cognitive radars, where the radar adapts its internal degrees of freedom in order to improve its capabilities [8]. Specific papers address the optimization of the waveform properties in order to improve the detection of the target or track properties [9], [10], [11]. These waveform properties are internal degrees of freedom of radars that include the polarization of the signal (already vastly used in weather radar and Synthetic Aperture Radar (SAR). Frequency diversity is also a tool to avoid detection or localization by adverse countermeasures [12]. Specific schemes of data fusion allow the usage of two simultaneous radar bands for tracking [13], ISAR imaging [14] and detection [15], [16]. The detection of changes or targets in multidimensional returns of the clutter has been addressed in SAR analysis [17], mainly in the context of polarimetric diversity. It allows the detection of changes in the properties of the clutter in either spatial or temporal dimension. The effective

rank of a matrix is a measure of the effective dimension of the space spanned by its action [18], and is used in SAR to count the main features of a signal. Clutter filtering has been shown to be more accurate when the effective rank of the covariance matrix of the clutter is low, i.e. when there are few scattering mechanisms [19], since the signature of the target can evolve in a greater dimensional space without being blurred by the clutter signature.

In this article, we study the properties of the clutter under the variations of both the polarization and the central frequency of the radar wave by doing actual clutter measurements in S-band. The covariance matrix of the clutter returns highlights the temporal variations of the signature of the clutter and the influence of the quality and quantity of the degrees of freedom on this signature. In particular, we compare the influence of the frequency and polarization degree of freedom on the effective rank of the covariance matrix of the clutter by the analysis of the measured signature of ground clutter. We show that the frequency and polarization degree of freedom seem to yield similar effective rank on strong clutter returns. We eventually study the impact of a bad estimation of the covariance matrix of the clutter on the false alarm rate through Monte-Carlo simulations based on real clutter data. A Maximum-Likelihood detector using the covariance matrix of a clutter cell is fed with synthetic data sampled with a covariance matrix of the same clutter cell at a different time. The change of the threshold needed to keep a constant false alarm rate gives information on the temporal stability of the clutter signature. The polarimetric behaviour of the clutter appears more stable than its frequency behaviour. This work proposes a framework to evaluate detectors and algorithms of endo-clutter target detections for ground radar through the usage of real data collection. Cognitive algorithms using multiple waveforms and degrees of freedom may use this framework since it provides evaluation tools based on real data.

2.0 METHODOLOGY

2.1 Experimental Setup and Pre-Processing

The experiments presented in this section use the HYCAM radar, an S-band demonstrator radar located in ONERA's site in Palaiseau. The experiments took place in 2024/02/08. The system is located on the top of a building allowing it to overlook many different environments. The HYCAM radar is a fully polarimetric radar with an instantaneous bandwidth of 500 MHz and a peak power of 1 kW [20]. In the experimental configuration, the radar aimed towards a specific clutter slice, which is the same as in [21]. However, in this experiment the aperture in azimuth was 4°. This clutter slice contains a very diverse set of clutters, including farmland, roads, buildings and forest. On the day of the experiment, it was raining so that some clutter cells contains signal from hydrometeors.

The experiments feature two different degrees of freedom of the radar: the polarization and the carrier frequency of the waveform. To do so, we use a composite signal built from several chirps with different characteristics. The sent signal is a periodic sequence of 8 linear chirps with a bandwidth of $B = 2\ MHz$, a pulse duration $\tau = 10\ \mu s$ and a spacing between the pulses of $100\ \mu s$. The first four chirps are transmitted in Horizontal (H) polarization and have the following central frequencies (in MHz around 3.15 GHz): 20, -7.5, 7.5, -20. The next four chirps use the same frequencies but are transmitted in Vertical polarization (V). The signal is received in both h and v polarizations. The whole pulse repetition interval (PRI) of the signal is $800\ \mu s$ due to this alternating pattern.

The radar continuously records the signal on two reception channels with polarisation h and v. The raw radar data are recorded at a sampling frequency of 50 MHz around 3.15 GHz in order to contain the signals of the four different chirps. The signals corresponding to each of the chirps are temporally extracted in a post-processing step and undergo a pulse compression with their replica, keeping only a window of 5 MHz around the central frequency. This allows separating the contribution of each of the frequency and polarization of the signals to build the multi-dimensional signature of the clutter. The data obtained is thus

composed of 16 channels (4 different frequencies in 4 different polarizations), containing radar data over a distance $D_m = \frac{c\Delta t}{2} \approx 15\ km$ at a resolution $\delta x = \frac{c}{2f_s} \approx 30\ m$. The channel index α contains the central frequency of the signal, the polarization of emission and reception of the signal. The sixteen channels are simultaneously recorded, but it is possible to select a subset of channels to perform the analysis as if only some channels are present.

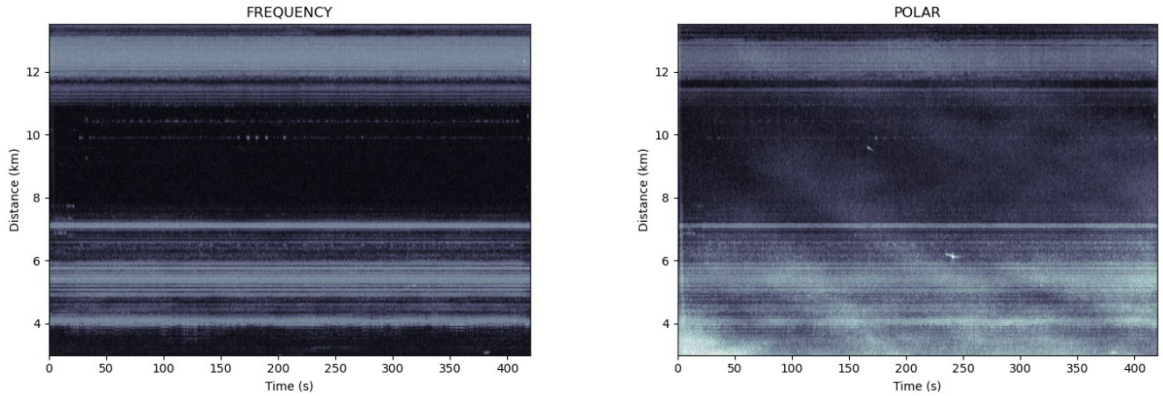

Figure 1: Time-distance maps of the low-speed signal. Left: Frequency degree of freedom. Right: Polarization degree of freedom.

The signal of the clutter is composed of the low-speed signal, which is obtained by Doppler filtering of the signal. Specifically, if the radar signal of a channel α at time $\tau_i^p = i * PRI$ and distance x is denoted by $s_\alpha(\tau_i^p, x)$, then the extraction of the signal around zero-speed of the channel α at time $\tau_j^d = j * N_d PRI$ is the mean of the signal s_α around this instant:

$$D_\alpha(\tau_j^d, x) = \frac{1}{N_d} \sum_{i=1}^{N_d} s_\alpha(\tau_j^d + \tau_i^p, x).$$

The clutter data is sampled with the time $t_d = 12\ ms$ over the duration of the measurement, corresponding to $N_d = 15$. The "zero-speed" zone corresponds to objects having a radial velocity between -4 and 4 m/s relative to the radar. To compute other specific speed cells of the signal, one uses the Fourier transform of the signal along the pulse axis and extracts the frequency corresponding to the wanted speed.

The covariance matrix $M_{\alpha\beta}(t, x)$ of the clutter signal at time t is computed using the Sample Covariance Matrix approach:

$$M_{\alpha\beta}(t, x) = \frac{1}{N_c} \sum_{j=1}^{N_c} D_\alpha(t + \tau_j^d, x) D_\beta^*(t + \tau_j^d, x)$$

The covariance is computed among the channels constituting the radar signal, and the average is computed on $N_c = 50$ samples. These signals are not recorded at the exact same time for each channel since the frequencies and the polarizations of emission change during the whole PRI of $800\mu s$. We make the hypothesis that this delay is negligible to the characterization of the clutter, which is a low speed and very wide object: with this resolution range, the azimuth aperture of 4° and a range of 10 km, the typical area of a cell is around 2ha.

2.2 Analysis of the Time Series of Covariance Matrices

The dimension of the covariance matrix is the number of degrees of freedom in the signal. Our experimental protocol allows tuning offline the diversity of the signal through channel selection. We can study the impact of two different diversities: polarization and central frequency. The polarimetric signature of the clutter has been studied in [22]. It features properties of stability with time and allows defining detectors harnessing the polarization degree of freedom to detect endo-clutter targets even at low Signal to Clutter Ratio. If some detectors are only affected by the amplitude of the signal, other detectors can use its multidimensional structure to filter out the signature of the clutter. A comparative study of these types of detectors is sketched in [21]. We propose to pursue the analysis of the covariance matrix of the clutter in order to study detectors sensitive to the multidimensional structure of the covariance matrix.

The covariance matrix of the clutter is a complex-valued array of size $N \times N$, so that it is suitable to reduce the dimensionality of the problem using simpler scalar quantities. The eigenvalues of the covariance matrix are common tools to study the elementary scattering mechanisms. These eigenvalues λ_a are positive real numbers since the covariance matrix is a semi-definite positive matrix. This allows defining the Shannon entropy of the eigenvalues of a covariance matrix $H(M) = -\sum_{a=1}^{N_{channel}} p_a \log(p_a)$, where $p_a = \frac{\lambda_a}{\sum_{a=1}^{N_{channel}} \lambda_a}$ is the normalized eigenvalue with index a. This entropy is linked to a quantity called the effective rank of a matrix, written $erank(M) = \exp(H(M))$, which is an empirical measure of the dimensionality of a matrix. Indeed, due to the presence of noise in the measurements, an empirical covariance matrix almost surely is of maximal rank. The effective rank quantifies how much the matrix action is dominated by its action on specific subspaces (eigenvectors). Some eigenvalues are so much larger than the others that the matrix mainly acts in the subspaces of these dominant eigenvectors. If the covariance matrix of the clutter has an effective rank near one, then the filtering of the clutter may be done by projecting out the dominant eigenvector. This filtering is more efficient when the effective rank is of one. The entropy and the effective rank can be computed for an arbitrary set of degrees of freedom. To do so, the eigenvalues and the effective rank are computed on a matrix with coefficients corresponding to specific degrees of freedom.

2.3 Detection of Endo-Clutter Targets

We want to study the filtering of the endo-clutter targets with the covariance matrices of the clutter. To do so, we use a Maximum Likelihood detector

$$f(X) = X^H M^{-1} X,$$

where X is the vector containing the radar data and M is the covariance matrix of the clutter. We empirically study the false alarm rate of this detector when the covariance matrix of the clutter is estimated at an instant different from the detection instant. The vector X is then sampled with a covariance matrix M'. It is expected that this deteriorates the false alarm rate of the detector since the hypothesis that X is sampled with the correct covariance matrix is no longer true. We compute the distribution of the values detector using Monte-Carlo simulation. We sample $N = 10000$ random vectors X distributed with a given complex covariance matrix and compute the threshold associated to a $P_{FA} = 10^{-2}$, which we denote as $T_{MM'} = q_{MM'}(1 - P_{FA})$, where $q_{MM'}(x)$ is the quantile function of the distribution of the test. The P_{FA} is high so that it is possible to perform faster numerical simulations and only to qualitatively grasp the effect of the covariance matrix mismatch. If the vector X is sampled with a covariance matrix sampled at another time than the matrix M, then the distribution of the test is different and the corresponding threshold is modified. This allows computing an empirical variation of the threshold as a function of time, which corresponds to the difference between the thresholds at a given time

$$\Delta T(M, M') = \frac{T_{MM'}}{T_{MM}}$$

Strong values of this threshold suggest that the clutter signature is not stable in time and can trigger additional false alarms only due to variations of the signature and not the presence of a target

3.0 RESULTS

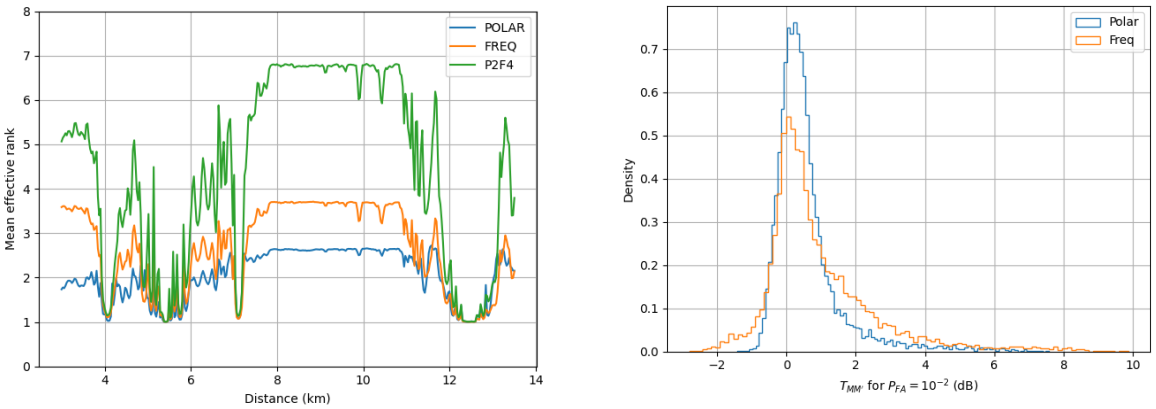

Figure 2: Left: Mean effective rank of the covariance matrix as a function of the distance. Right: Distribution of the modified threshold to guarantee $P_{FA} = 10^{-2}$ when using the covariance matrix with a time delay.

To characterize the endo-clutter detection in this low-grazing environment, we study the time variations of the effective rank of the covariance matrices. For both strong clutter returns and targets, we expect that it shall be around one since there is a clear mechanism of scattering. We analyse the time-distance map of this effective rank of the signal at low speed to provide a visualization of this region of the signal. Figure 1 features two estimations of the effective ranks of covariance matrices using different degrees of freedom: central frequency and polarization of the waveform. In the left figure, only the Hh polarization is kept for the four central frequencies whereas in the right figure only the first frequency is kept for the three polarizations (Hh, Vh, Vv). This figure is computed by averaging the effective ranks of the signal contained in the three clutter cells with speed between -12m/s and +12 m/s. It was raining on the day of the experiment, and the figures show that the rain is more apparent using the polarization degree of freedom, which is consistent with the usage of polarization by weather radar. It can also be seen that some specific bright signals – likely low-speed targets – are not apparent with the frequency degree of freedom whereas they are using the polarization degree of freedom. This effective rank analysis yields an interesting visualization of the complex and evolving environment surrounding the radar, and helps identifying the regions with strong clutter returns. We can also identify ranges featuring targets.

Figure 2 left shows the evolution of mean effective rank of the covariance matrix of the clutter with the distance. In this case, only the zero-speed clutter range cell is kept, and the mean is computed over the whole time of the experiment. Three sets of parameters are used to compute this effective rank: POLAR, FREQ and P2F4 which respectively designs the polarimetric degrees of freedom (Hh, Vh, Vv), the frequency degree of freedom, and a combination of two polarizations (Hh, Vh) and four frequencies. The effective ranks show variations and are close to one for high values of clutter returns. On the contrary, a pure noise with the same amplitude in all channels has an effective rank equal to the number of channels. The frequency degree of freedom seems to yield smaller effective ranks on some range cells but is subject to stronger variations with distance. The P2F4 combination of degree of freedom indeed yields low ranks for strong clutter returns but

its effective rank strongly increases when there is no more clutter signal. The POLAR and FREQ degree of freedom respectively saturates around effective rank 3 or 4 in the presence of noise, consistently with their number of degrees of freedom. An effective rank near one shall represent a guarantee that the filtering of the signature can be done in a very efficient way using the detector presented.

Figure 2 on the right shows the impact of the mismatch of the covariance matrix on the threshold of false alarm $\Delta T(M, M')$ for a $P_{FA} = 10^{-2}$. To do so, we choose a specific reference time t_0 to estimate the covariance matrix $M(d, t_0)$ at each distance d. Then, for each distance, we compute the covariance matrix $M'(d, t_i)$ for a wide set of time t_i covering the duration of the experiment. We generate random data under the covariance matrix $M'(d, t_i)$ and make detections using $M(d, t_0)$, and compute the 10^{-2} quantile of the distribution, which yields our quantity $\Delta T(M(d, t_0), M'(d, t_i))$. To assess the impact of the degrees of freedom on the false alarm rate, we aggregate all the distances and times and study the histograms of the quantity $\Delta T(M, M')$ for the two different diversities "POLAR" and "FREQ". This histogram approach averages very different types of phenomena: ranges with only noise, ranges with strong clutters, ranges and time with incidental targets… Overall, the distribution of this quantity is less wide for the polarization than for the frequency degree of freedom. It seems to indicate that the polarimetric signature is more stable. A more detailed time analysis of this threshold is not presented here, but shows strong and non-monotonic time fluctuations of $\Delta T(M(d, t_0), M'(d, t))$ in cells containing strong clutter returns for both diversities. Strong time variations of the threshold are problematic since they risk inducing strong false alarm rates if the covariance matrix of the clutter is not updated frequently enough. However, each estimation of the covariance matrix of the clutter may include coincidental endo-clutter targets, which is specifically what the detector seeks to detect and does not want to filter out. It may be of interest to adapt the threshold of false alarm to these variations and to accept a degradation in performance, provided this do not deteriorate too much the performances of detection. This study shall be completed by a more extensive study of the signature of targets in this configuration.

4.0 CONCLUSION

The impact of the degrees of freedom used by a ground radar to measure clutter in a low-grazing geometry is analysed under the light of the effective rank of the covariance matrix of the clutter. This analysis yields a nice visualization tool of the data in time and distance for low-speed signals, and shows in particular that hydrometeors signal are filtered by the frequency degree of freedom but are visible using the polarization degree of freedom. Some low-speed target signals are not as much apparent using the frequency or polarization degree of freedom. A distance analysis of the effective rank show that it is similar for the frequency and for the polarization degree of freedom. A complemental analysis on the variations of the covariance matrices is performed on specific clutter range cells. It shows that the covariance matrix of the clutter needs to be frequently estimated to keep a constant false alarm rate. In this respect, the frequency signature of the clutter seems to be less stable than the polarimetric signature. Building detectors that are more robust may involve specific detection algorithms or estimation schemes for the covariance matrices, since a too frequent estimation of the covariance matrices is subject to other problems such as the presence of a target in the clutter cells. Acquisition of real target signals with various waveform diversities can offer a more complete vision of possible algorithms which tune the radar degrees of freedom. The inclusion of degrees of freedom such as the bandwidth or PRI might also be of interest.

5.0 REFERENCES

[1] Wellig, P., Speirs, P., Schuepbach, C., Oechslin, R., Renker, M., Boeniger, U., & Pratisto, H. (2018, June). Radar systems and challenges for C-UAV. In 2018 19th International Radar Symposium (IRS) (pp. 1-8). IEEE.

[2] Tahmoush, D. (2015). Review of micro-Doppler signatures. IET Radar, Sonar & Navigation, 9(9), 1140-1146.

[3] Hoffmann, F., Ritchie, M., Fioranelli, F., Charlish, A., & Griffiths, H. (2016, May). Micro-Doppler based detection and tracking of UAVs with multistatic radar. In 2016 IEEE radar conference (RadarConf) (pp. 1-6). IEEE

[4] Li, Y., Zhang, G., & Doviak, R. J. (2013). Ground clutter detection using the statistical properties of signals received with a polarimetric radar. IEEE Transactions on Signal Processing, 62(3), 597-606.

[5] Maniraguha, F., Vodacek, A., Ndashimye, E., & Rushingabigwi, G. (2021, October). Ground Clutter Mitigation and Insect Signature Detection for Polarimetric C-Band Doppler Weather Radar. In 2021 IEEE Global Humanitarian Technology Conference (GHTC) (pp. 289-296). IEEE.

[6] Friedrich, K., Germann, U., & Tabary, P. (2009). Influence of ground clutter contamination on polarimetric radar parameters. Journal of Atmospheric and Oceanic Technology, 26(2), 251-269

[7] Ezuma, M., Anjinappa, C. K., Funderburk, M., & Guvenc, I. (2021). Radar cross section based statistical recognition of UAVs at microwave frequencies. IEEE Transactions on Aerospace and Electronic Systems, 58(1), 27-46.

[8] Haykin, S. (2006). Cognitive radar: a way of the future. IEEE signal processing magazine, 23(1), 30-40.

[9] Smith, G. E., Cammenga, Z., Mitchell, A., Bell, K. L., Johnson, J., Rangaswamy, M., & Baker, C. (2016). Experiments with cognitive radar. IEEE Aerospace and Electronic Systems Magazine, 31(12), 34-46.

[10] Oechslin, R., Aulenbacher, U., Rech, K., Hinrichsen, S., Wieland, S., & Wellig, P. (2017, October). Cognitive radar experiments with CODIR. In International Conference on Radar Systems (Radar 2017) (pp. 1-6). IET.

[11] Oechslin, R., Wieland, S., Hinrichsen, S., Aulenbacher, U., & Wellig, P. (2019). A cognitive radar testbed for outdoor experiments. IEEE Aerospace and Electronic Systems Magazine, 34(12), 40-48.

[12] Moon, T., Park, J., & Kim, S. (2022). BlueFMCW: Random frequency hopping radar for mitigation of interference and spoofing. EURASIP Journal on Advances in Signal Processing, 2022(1), 1-17.

[13] Brenner, T., Hardejewicz, J., Rupniewski, M., & Nalecz, M. (2012, May). Signals and data fusion in a two-band radar. In 2012 13th International Radar Symposium (pp. 15-18). IEEE.

[14] Cerutti-Maori, D., Rosebrock, J., Carloni, C., Budoni, M., Maouloud, I., & Klare, J. (2021). A novel High-Precision Observation Mode for the Tracking and Imaging Radar TIRA–Principle and Performance Evaluation. In 8th European Conference on Space Debris, ESA/ESOC, Darmstadt, Germany, Virtual Conference.

[15] Fante, R. L. (1996). Multifrequency detection of a slowly fluctuating target. *IEEE transactions on aerospace and electronic systems*, *32*(1), 495-497.

[16] Vannicola, V. (1974). Detection of slow fluctuating targets with frequency diversity channels. *IEEE Transactions on Aerospace and Electronic Systems*, (1), 43-52.

[17] Conradsen, K., Nielsen, A. A., Schou, J., & Skriver, H. (2003). A test statistic in the complex Wishart distribution and its application to change detection in polarimetric SAR data. *IEEE Transactions on Geoscience and Remote Sensing*, *41*(1), 4-19.

[18] Roy, O., & Vetterli, M. (2007, September). The effective rank: A measure of effective dimensionality. In *2007 15th European signal processing conference* (pp. 606-610). IEEE.

[19] Brennan, L. E., & Staudaher, F. M. (1992). *Subclutter visibility demonstration*. Tech. Rep., RL-TR-92-21, Adaptive Sensors Incorporated.

[20] Brouard, P., Constancias, L., Brun, A., Attia, S., Peyret, J., & Dreuillet, P. (2013). Hycam: A new S band surface radar testbed.

[21] Rozel, M., Bruneel, P., Brouard, P., & Oriot, H. (2022). Influence of covariance matrix mismatch on polarimetric detectors for low-grazing endo-clutter detection.

[22] Polarimetric detection of endo-clutter UAV in a low-grazing geometry, Milan Rozel (PhD Thesis, to be published)